CIRCUITS SYSTEMS SIGNAL PROCESS
VOL. 19, NO. 6, 2000, PP. 549–566

VECTOR FITTING BY POLE RELOCATION FOR THE STATE EQUATION APPROXIMATION OF NONRATIONAL TRANSFER MATRICES*

Adam Semlyen[1] *and Bjørn Gustavsen*[2†]

Abstract. Often the information available for a state equation description in the form $\dot{x} = Ax + Bu$, $y = Cx + Du$ is via a transfer function matrix $H(s)$ obtained by measurements or complicated computations for frequencies $s = j\omega$. Thus $H(s)$ is nonrational or rational of high order. Its state equation approximation means obtaining A, B, C, D in the rational transfer matrix $C(sI - A)^{-1}B + D \approx H(s)$. This approximation problem is difficult because it is nonlinear and often ill conditioned. This paper describes a methodology for fitting the columns $h(s)$ of $H(s)$ by two linear procedures. First $\theta(s)h(s)$ is fitted with a set of prescribed poles, where $\theta(s)$ is an unknown rational function with the same poles as $\theta(s)h(s)$. Then the poles for $h(s)$ are calculated as the zeros of $\theta(s)$. With the poles known, the unknown residues and constant terms are calculated for $h(s)$. If necessary, the procedure is repeated with the new poles taken as prescribed poles. The procedure is accurate and robust, and uses only standard numerical linear algebra computations.

Illustrative examples for the application of vector fitting are given for a power transformer, a transmission line, and a network of transmission lines.

Key words: Rational approximation, rational fitting, state equations, transfer function, transmission lines, poles, residues.

1. Introduction

It is customary to use state equations in the standard form

$$\dot{x} = Ax + Bu, \qquad y = Cx + Du \tag{1}$$

for linear parts of dynamic systems. In the applications of interest to us, (1) is the form used for the modeling and simulation of transmission lines, transformers,

* Received June 8, 1999; revised May 5, 2000. This work received financial support by the Natural Sciences and Engineering Research Council of Canada and by SINTEF Energy Research, Norway.

[1] Department of Electrical and Computer Engineering, University of Toronto, Toronto, Ontario, Canada M5S 3G4. E-mail: adam.semlyen@utoronto.ca

[2] SINTEF Energy Research, N-7465 Trondheim, Norway.
E-mail: bjorn.gustavsen@energy.sintef.no

† The Matlab code of Vector Fitting is freely available from the second author.

and external system equivalents for the calculation of electromagnetic transients in power systems. In all cases, the information available is in the form of a frequency domain transfer function matrix $H(s)$, $s = j\omega$, obtained either by computation (overhead lines, cables, external systems) or measurements (transformers). Thus $H(s)$ is not rational, but (1) leads to a rational matrix for its approximation:

$$H(s) \approx C(sI - A)^{-1}B + D. \tag{2}$$

Our purpose is to obtain the matrices A, B, C, D for a low-order state equation approximation (1) such that (2) is satisfied with high accuracy over a wide range of frequencies ω. The given transfer matrix $H(s)$ is either nonrational or it could be rational of high order. In the latter case, the result is an order-reduction technique.

In the field of applications we have mentioned, it is often the case (e.g., in overhead lines [9], [17]) that $H(s)$ is diagonalizable with transformation matrices that are real and almost constant. Then (2) leads to scalar (modal) subproblems. Many of the existing publications [9], [11], [17], [20] dealt originally with the modal problem formulation or used it as a first step [3], [6], [10] to the complete (phase-domain) analysis [1], [13], [14], [18], [19]. Some recent work [1], [3], [5], [13], [14], [18], [19] has addressed the problem in its complete form (2). Our contribution to this topic consists in the development of a new methodology, *vector fitting* [4], [7], that is both practically useful and theoretically interesting. It is applicable to both modal and phase-domain analysis. Because the theoretical aspects of the new methodology have not yet been analyzed, we will address these in the present paper.

The basic idea of vector fitting by pole relocation (VFPR) is that the nonlinear and notoriously ill-conditioned problem of rational approximation (2) can be dealt with in an efficient way if we do not attempt to find poles for fitting the columns $h(s)$ of $H(s)$ but mold $h(s)$ into a new vector $g(s) = \theta(s)h(s)$, where $\theta(s)$ is an unknown shaping function that makes it possible to fit $g(s)$ using predefined poles. Thus A in (2) becomes known, and if the columns of B are normalized, then only C and D remain unknown in (2). The end result is a very robust procedure. Its MATLAB code is freely available from the second author.

In order to introduce the new method, in Section 2, we give a characterization of the problem of state equation approximation (SEA). Then in Section 3, we describe the new methodology, vector fitting by pole relocation.

2. Characterization of the state equation approximation problem

2.1. Basic remarks

For simplicity of presentation, we remove the term D in (1) and (2). The elements of $H(s)$ in (2) are rational polynomials with common poles p_j, the roots of

$\det(sI - A)$. Any column $h(s)$ of $H(s)$ can be written as

$$h(s) \approx C(sI - A)^{-1}b, \tag{3}$$

where b is the corresponding column of B. Note that normally A in (3) can be chosen diagonal via a similarity transformation. Then, for additional simplification, its elements are assumed to be complex conjugate (the poles p_j and p_j^*). We can normalize b to "ones" by appropriately scaling the corresponding columns of C. Then any element of $h(s)$, or the vector (or scalar) $h(s)$ itself, takes the form

$$h(s) \approx \sum_j \frac{r_j}{s - p_j} + \sum_j \frac{r_j^*}{s - p_j^*}, \tag{4}$$

where the residues r_j and r_j^* are scalars or vectors, depending on $h(s)$. We can thus make the following remarks.

Remark 1. If A is unknown, then the SEA is a nonlinear problem in the unknowns. If A is known, then the SEA becomes a linear problem.

Remark 2. Separating $H(s)$ into its columns permits us to remove the elements of B from the unknowns. If in addition A is known, then the only unknowns in (4) are the residues r_j (which correspond to the elements of C).

Remark 3. All elements in a column $h(s)$ share the same poles.

With $s_i = j\omega_i$, (4) can be written in the form

$$\underbrace{\begin{bmatrix} \vdots \\ h(s_i) \\ \vdots \end{bmatrix}}_{h} \approx \underbrace{\begin{bmatrix} \cdots & \vdots & \vdots & \cdots \\ & \frac{1}{s_i - p_j} & \frac{1}{s_i - p_j^*} & \\ & \vdots & \vdots & \end{bmatrix}}_{G} \underbrace{\begin{bmatrix} \vdots \\ r_j \\ r_j^* \\ \vdots \end{bmatrix}}_{r}. \tag{5}$$

Note the resemblance of G with the Hilbert matrix, with elements $H_{i,j} = 1/(i + j - 1)$, and even more with the Cauchy matrix (with elements $C_{i,j} = 1/(x_i + y_j)$, where $x_i, y_j \in R$, and of which the Hilbert matrix is a special case; see [8, p. 515]; see also [15], [16]) which are known to become very ill conditioned with increasing size. Therefore, we expect that G too is ill conditioned. This will indeed be the case.

Matrix G in (5) is a "basis" matrix related to the calculation of the residues r. The poles could also be calculated from (5) using nonlinear optimization. This would require linearization of G with respect to the poles, which leads to a basis matrix G' for the increments Δp_j, Δp_j^* of the poles:

$$G' = \begin{bmatrix} \cdots & \vdots & \vdots & \cdots \\ & \frac{r_j}{(s_i - p_j)^2} & \frac{r_j^*}{(s_i - p_j^*)^2} & \\ & \vdots & \vdots & \end{bmatrix}. \tag{6}$$

This too turns out to be just as ill conditioned as G. Consequently, we state that

Remark 4. Both the calculation of residues for given poles and of the poles themselves—which is anyway a difficult task because of nonlinearity—is fraught by ill conditioning.

2.2. *Singular-value decomposition: Analysis*

The effect of ill conditioning can be conveniently analyzed by singular-value decomposition (SVD) of the basis matrices G and G' of (5) and (6). This yields, for example for (5),

$$G = USV^* \quad \text{and} \quad h \approx Gr = USV^*r = USq \qquad (r = Vq), \tag{7}$$

where U is a unitary basis matrix for h consisting of orthonormal vectors u_k, and S is the diagonal matrix of the singular values σ_k of G, in decreasing order. V also is unitary. The following remarks are now in order.

If we solve (7) for q, as σ_k decreases so will q_k become accordingly larger. It is therefore customary (in order to avoid catastrophic numerical cancelations) to remove from the SVD the part related to extremely small singular values. We note however that to the extent that large values exist in the vector q, the residues r $(= Vq)$ will also become large (because V is unitary). But a good rational fitting (4) should certainly be obtained (unless a pole is very large) with residues as small as possible! Therefore, we conclude that

Remark 5. Good rational approximations are predicated on the possibility of their realization with small residues.

Remark 6. A vector h can be satisfactorily fitted (by the above requirement), when G in (7) is indeed ill conditioned, only if it is in the range of the first few columns of U, i.e., if we can obtain it with small values q_k:

$$h \approx \sum_k u_k \sigma_k q_k. \tag{8}$$

2.3. *SVD: Examples*

Two situations will be considered in the following, according to whether all poles are or are not well away from the imaginary axis.

Case A: No poles close to the imaginary axis.

Figure 1 gives the singular values σ_k of the basis matrices G and G' of (5) and (6) for two pole distributions. The location of the poles is shown in the left subplots. There are 5×5 poles in each case, plus their conjugates. In the upper plot, the poles

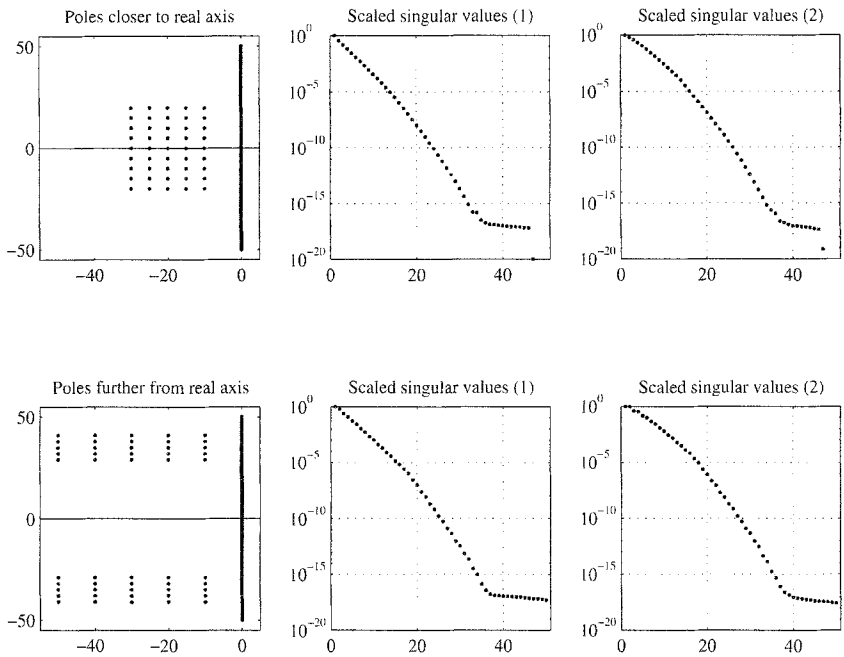

Figure 1. Singular values of matrices G and G' for two pole distributions away from the imaginary axis.

are closer to the real axis (the lower row is on the axis), whereas in the lower plot the poles are further away. Thus we have two distinct patterns with the common feature that no pole is close to the imaginary axis. There are 101 equidistant frequency points on the imaginary axis (including the one at the origin), and they are shown in the figure. 50 points correspond to positive and 50 to negative frequencies. The requirement for considering negative, as well as positive, frequencies stems from the fact that $h(s)$ of (4) has the property $(h(s))^* = h(s^*)$ (because its poles and residues come in conjugate pairs). Therefore, if a partial fraction expansion is valid and accurate for $h(s)$ at positive frequencies ($s = j\omega$, $\omega > 0$), then it must be valid also for $(h(s))^*$ and thus for $h(s^*)$, i.e., for negative frequencies. With these details, the results are readily reproducible.

The middle subplots give the singular values of G. They are scaled such that the first singular value is 1. The right subplots give the singular values of G' where all residues, r_j and r_j^* in (6), are assumed to be 1. We note that, irrespective of the pole distribution, both matrices are very ill conditioned, and the details of the pole distributions make almost no difference. Similar results are obtained with randomly chosen poles. The ill conditioning is such that in double-precision calculations (e.g., in MATLAB) all but at most the first 25 singular values should be set to zero. However, as pointed out in Remark 6, only a few singular values

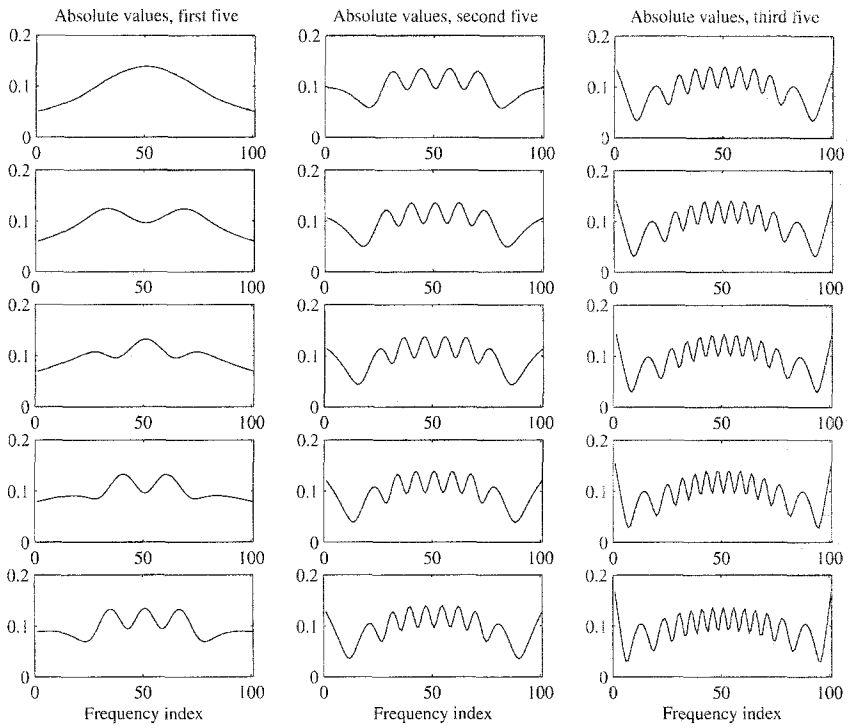

Figure 2. Mode shapes of the absolute values of the first 15 columns of U for the basis matrix G.

and, accordingly, only the first few vectors of U (singular vectors or modes of G) should be kept for good rational fitting. This has the following implications.

The mode shapes (plots of the singular vectors u_k of the basis matrix G against the corresponding 101 frequency points) become more and more oscillatory as k increases. This is shown in Figure 2 for the first 15 modes corresponding to the upper plots of Figure 1. We can see that the number of oscillations is roughly proportional to the order k of the mode. For the lower plots of Figure 1, we obtain similar results regarding the increase of the number of oscillations in the mode shapes with increasing k. Because the first modes are smooth and the oscillatory ones contribute less and less to h in (8) as σ_k becomes smaller, h must itself be fairly smooth for a good fitting. Thus, unless very large residues are permitted, we note that

Remark 7. Only smooth functions h can be fitted with poles that are not close to the imaginary axis.

If the residues are to be kept small, for instance if in (8) for $k \geq 2$ and $K > 1$ (e.g., $K = 3$) we require that

$$|q_k| < K|q_1|, \tag{9}$$

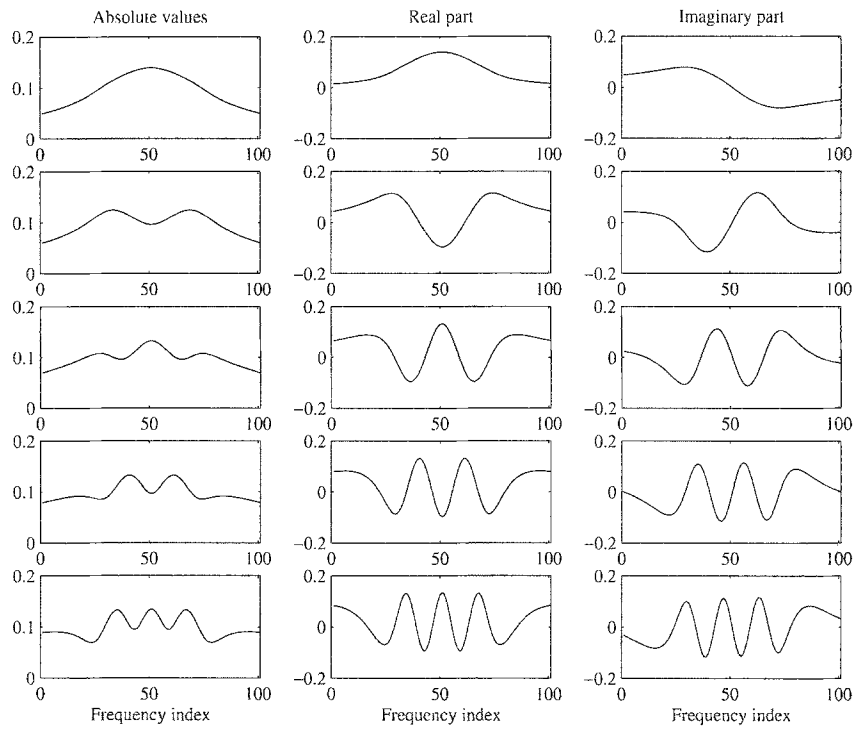

Figure 3. Mode shapes, including real and imaginary parts, of the first five columns of U for the basis matrix G.

then, taking into account the fast decrease of σ_k shown in Figure 1, h obtained from (8) will be confined to a not too wide band, defined by only a few modes u_k ($k \geq 2$) around the first singular vector u_1. Figure 3 shows (for the upper part of Figure 1) the absolute values and the real and imaginary parts of the first five mode shapes u_k of G. Then, based on (8) and (9) and normalizing q_1 to 1, these are combined according to

$$h_{\text{real/imag}} = u_{1\text{real/imag}}\sigma_1 \pm K \sum_{k=2}^{k_{\max}} u_{k\text{real/imag}}\sigma_k \tag{10}$$

to give the upper and lower limits for (the real and imaginary parts of) h. These are shown (for several $k_{\max}$), for the upper part of Figure 1, in the left half of Figure 4. For the lower part of Figure 1, these limits are shown in the right half of Figure 4.

We note now that, whereas the singular values shown in Figure 1 depend very little on the distribution of poles, the mode shapes do depend on the pole distribution even if their features of smoothness and oscillations are similar. Therefore,

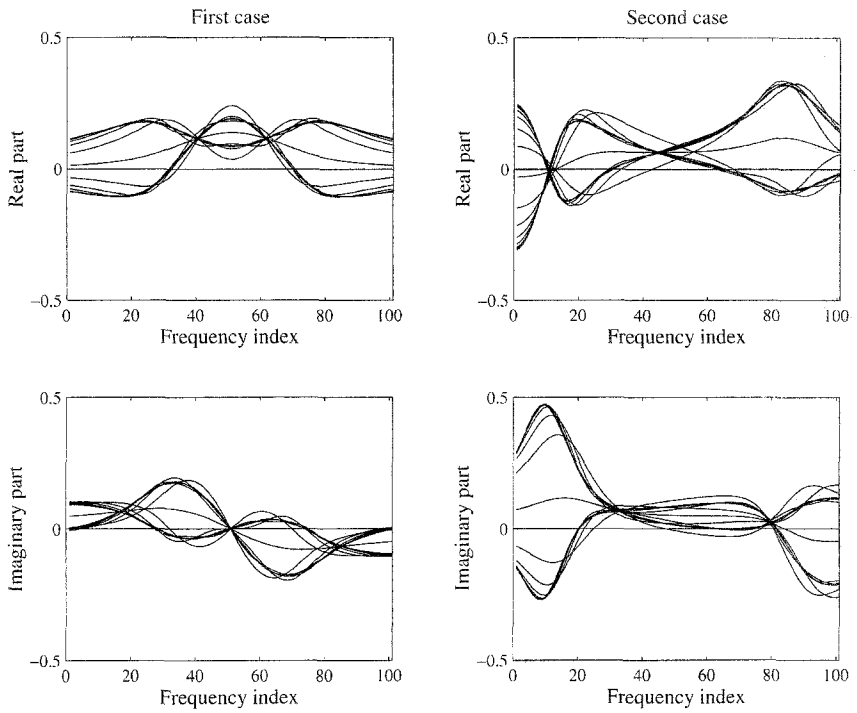

Figure 4. Upper and lower limits (for several $k_{\max}$) for h that can be fitted with the two-pole distributions of Figure 1.

the functions h that can be fitted are different, as shown in Figure 4. The result is that

Remark 8. Any given set of poles determines a limited range within which a function h can be fitted.

Thus,

(a) On one hand, for a given h, a set of poles cannot be located, due to the ill conditioning of G'. Also, from a larger set of given poles one cannot select a convenient subset for fitting by calculating the residues in (4), due to the ill conditioning of G in (5).
(b) On the other hand, by Remark 8, a function h cannot be fitted with predefined poles, unless it happens to be in their fitting range. In any case, with n singular vectors, only n points of h can be reached exactly.

Our solution to this dilemma is, as mentioned, to mold $h(s)$ into a new vector $g(s) = \theta(s)h(s)$, which is in the range of a chosen set of poles. Before showing (in Section 3) how this is done, we discuss another particular case of pole distribution.

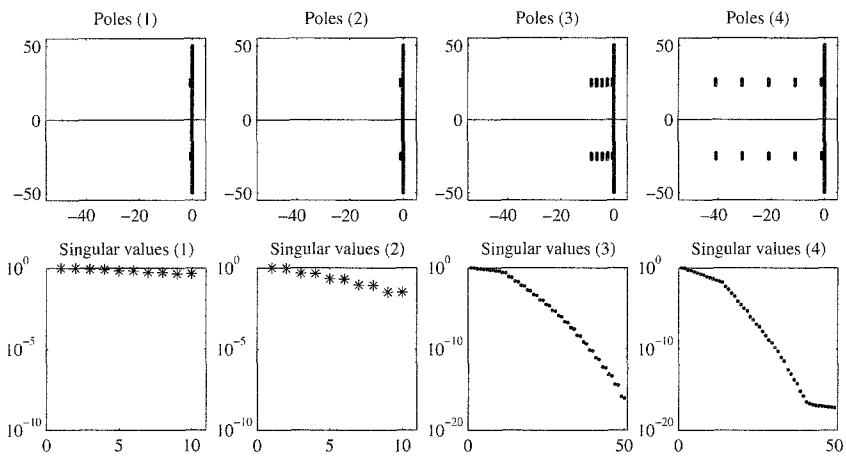

Figure 5. Singular values for four sets of poles close to the imaginary axis.

Case B: Some poles close to the imaginary axis.

Figure 5 shows the relative (with respect to σ_1) singular values for four pole distributions with at least some poles close to the imaginary axis. The location of the poles is shown in the upper subplots (but with the scale of the figure the vertical separation between poles is not distinguishable). There are 101 frequency points (including the conjugates), as before. In the first two cases there are 5 poles (plus their conjugates): in Case 1 their distance d to the imaginary axis is 0.2, in Case 2 it is 1. In Case 3 and Case 4, four more sets of poles have been added to the previous two cases (to a total of 25, plus their conjugates), respectively, distanced by $10d$.

The pattern of singular values shows in all cases that the first 10 decrease more slowly than the rest. This is related to the 10 poles (including the conjugates) that are close to the imaginary axis. The singular values for the second set of poles in Figure 5 come in almost equal pairs corresponding to the poles and their conjugates. (If only positive frequencies were used, then only five singular values would decrease slowly because the conjugate poles are not close to the points of observation on the positive branch of the imaginary axis.) The smaller the distance d of the poles to the imaginary axis, the slower is the decrease. The presence of additional poles in Cases 3 and 4 does not make much difference, except that there are now more singular values. When d is really small (in Cases 1 and 3, $d = 0.2$), the first 10 singular values are nearly equal.

Consequently, the first 10 singular vectors may potentially constitute a good basis for obtaining a given vector h, and more singular vectors are available for this purpose than in the case of poles that are all far from the imaginary axis (Figure 1). However, as shown in Figure 6, the first five mode shapes, represented against the 101 frequency points (including the negative frequencies), have their

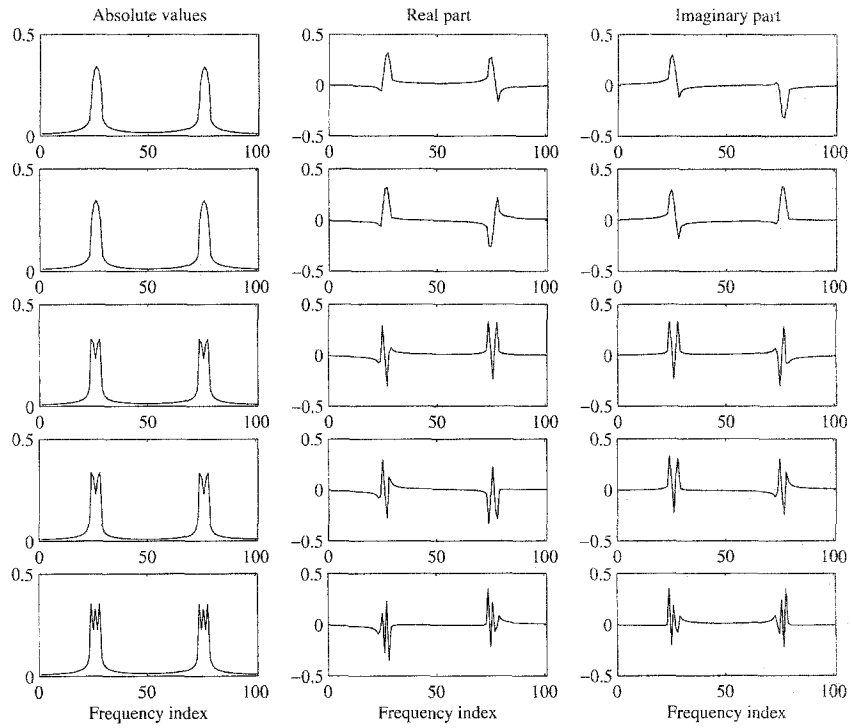

Figure 6. Mode shapes of the first five columns of U for the basis matrix G, Case 3 of Figure 5.

main variation concentrated to the vicinity of the five poles close to the imaginary axis. This, of course, is intuitively clear. The consequence of this fact is that the fitting of functions h with sharp variations is fraught with less ill conditioning than that of more general functions. However, it may still not be easy to locate the poles that would give a very good fit. Because of this, the method of pole relocation to be described in the next section is of practical significance even in this case.

3. Vector fitting by pole relocation

3.1. Procedure

Our objective is to calculate the unknown poles a_j, residues c_j, and the constant term d in the expression

$$h(s) \approx \sum_{j=1}^{N} \frac{c_j}{s - a_j} + d, \tag{11}$$

where $h(s)$ can be a vector or a scalar. To explain the method, we now assume that $h(s)$ is a scalar. The summation limit N is the order of the approximation, assumed to be known.

We recall that the difficulty in fitting $h(s)$ is due to the (unknown) poles a_j which appear in the denominator, thus causing (11) to become a nonlinear problem in the unknowns. However, if the poles had been known, then (11) would have been linear in the unknowns c_j, d, which could then have easily been calculated by solving a linear, least-squares problem.

Vector fitting solves (11) in two steps. Each step amounts to solving a linear system of the same form as (11), but with known poles.

Step 1: Pole identification.

Instead of fitting $h(s)$ directly, $h(s)$ is multiplied with an unknown rational function $\theta(s)$ of order N:

$$\theta(s) = \sum_{j=1}^{N} \frac{\hat{c}_j}{s - \bar{a}_j} + 1. \tag{12}$$

The poles of $\theta(s)$ are assigned a set of initial values $\bar{a}$, which span in an almost arbitrary way the domain of interest (see Section 3.2 for details). We then postulate that the function $\theta(s)h(s)$ can be fitted with the same set of poles $\bar{a}$ as $\theta(s)$:

$$\theta(s)h(s) = \sum_{j=1}^{N} \frac{\tilde{c}_j}{s - \bar{a}_j} + \tilde{d}. \tag{13}$$

Combining (12) and (13) gives

$$\left(\sum_{j=1}^{N} \frac{\hat{c}_j}{s - \bar{a}_j} + 1 \right) h(s) = \sum_{j=1}^{N} \frac{\tilde{c}_j}{s - \bar{a}_j} + \tilde{d}. \tag{14}$$

Equation (14) is linear in the unknowns $\hat{c}_j, \tilde{c}_j, \tilde{d}$, which are calculated by solving a linear least-squares equation of the form $Ax = b$.

From (14) we get

$$h(s) = \frac{\sum_{j=1}^{N} \frac{\tilde{c}_j}{s-\bar{a}_j} + \tilde{d}}{\sum_{j=1}^{N} \frac{\hat{c}_j}{s-\bar{a}_j} + 1} = \frac{\prod_{j=1}^{N} \frac{(s-\tilde{z}_j)}{(s-\bar{a}_j)}}{\prod_{j=1}^{N} \frac{(s-\hat{z}_j)}{(s-\bar{a}_j)}} = \frac{\prod_{j=1}^{N} (s - \tilde{z}_j)}{\prod_{j=1}^{N} (s - \hat{z}_j)}. \tag{15}$$

It is seen from (15) that the initial poles $\bar{a}_j$ cancel out, and that *the zeros* $\hat{z}_j$ *of* $\theta(s)$ *become the poles of* $h(s)$*!* The zeros of $\theta(s)$ are calculated by input/output interchange from its state equation obtained from (12) (see [7] for details).

Step 2: Residue identification.

With the poles of $h(s)$ known from Step 1, (11) is solved with respect to the unknown residues c_j and constant term d by solving a linear least-squares problem of the type $Ax = b$.

Steps 1 and 2 may have to be repeated several times with the new poles as starting poles, in order for the method to converge. As convergence is achieved, $\theta(s)$ becomes unity (i.e., all $\hat{c}_j$ become zero). With a good set of starting poles, we usually need fewer than five iterations for our applications. Thus, vector fitting solves (11) as follows.

1. Choose a set of starting poles $\bar{a}_1 \ldots \bar{a}_N$.
2. Solve (14) with respect to $\hat{c}_j, \tilde{c}_j, \tilde{d}$.
3. Calculate the poles $a_1 \ldots a_N$ of $h(s)$ as the zeros of $\theta(s) \cdot \theta(s)$ is given by (12).
4. Solve (11) with respect to c_j, d.
5. If necessary, repeat procedures 1–4 with the new poles as starting poles.

Details regarding the implementation are given in [7].

3.2. *Starting poles*

In general, iterations are needed to shift the starting poles into their final positions. Generally, the farther away the starting poles are from their final positions, the more iterations are needed.

Assume that $h(s)$ is to be fitted in the range ω_1–ω_2. The starting poles should be chosen as complex conjugate pairs with weak attenuation (e.g., $|\mathrm{Re}\{\bar{a}_j\}|/|\mathrm{Im}\{\bar{a}_j\}| = 0.01$) and linearly spaced over the considered frequency range ω_1–ω_2. This selection of starting poles gives a basis $G(s)$ in (5) which is usually well conditioned. This has the effect of reducing the required number of iterations.

In some applications, a different choice of starting poles may be advantageous. For instance, in transmission line modeling based on modes [9], [17], it is known a priori that the final poles are usually real and approximately logarithmically spaced. We then use real, logarithmically spaced starting poles, as a faster convergence is then achieved.

3.3. *Robustness and ill conditioning*

In order for the rational approximation to be useful for time-domain simulations, all poles have to be stable. If, for some reason, an unstable pole is calculated, we simply invert the sign of the real part before proceeding with the residue calculation. Typically, unstable poles occur during the first few iterations but vanish as convergence is achieved.

VFPR relies on solving two linear problems of the form $Ax = b$, with A corresponding to G in (5). In the following, we explain the fact that VFPR remains a robust procedure, also when A is ill conditioned.

Typically, A is ill conditioned when there are many real poles. When fitting a function using real starting poles, the residues calculated in the first step of VFPR are slightly inaccurate, and so the new poles become inaccurate. However, if the function we are trying to fit is smooth (has real poles only), then the new poles will still give a good fitting because the accuracy of the fitting is then only weakly dependent on exact pole locations.

On the other hand, when fitting a function containing many peaks (due to complex poles), the use of real starting poles gives a set of new poles that cannot yield a good fitting. But as shown in [7], some of the new poles are accurate (and complex). By repeating the fitting procedure with the new poles as starting poles, more and more poles become accurately located as the increased presence of complex poles with weak attenuation gradually removes the ill conditioning. Thus, after several iterations, accurate fitting is achieved. However, using complex starting poles as recommended in Section 3.2, A becomes well conditioned from the beginning, and convergence is obtained in only a few iterations. Thus, in general, VFPR is a very robust procedure for the fitting of functions containing real or complex poles, or both.

3.4. Overview

We have the following important result of pole relocation.

Remark 9. The original, very approximate, poles are replaced by the zeros of the shaping function $\theta(s)$ which can be easily calculated by input/output interchange in the state equations.

Based on Remarks 3 and 9, we can now describe the essential features of VFPR as follows.

Remark 10. VFPR achieves a column-wise state equation approximation of a nonrational transfer matrix that resembles traditional minimal realizations. It is well conditioned because the poles are not initially handled as unknown but are reassigned in a robust way by basic procedures of numerical linear algebra.

With these 10 remarks (results, and rules), the presentation of VFPR is now complete.

3.5. Examples

Example 1: Recovering the Coefficients of a Rational Scalar Function.

Consider the function

$$f(s) = \frac{2}{s+5} + \frac{30 + j40}{s - (-100 + j500)} + \frac{30 - j40}{s - (-100 - j500)} + 0.5. \qquad (16)$$

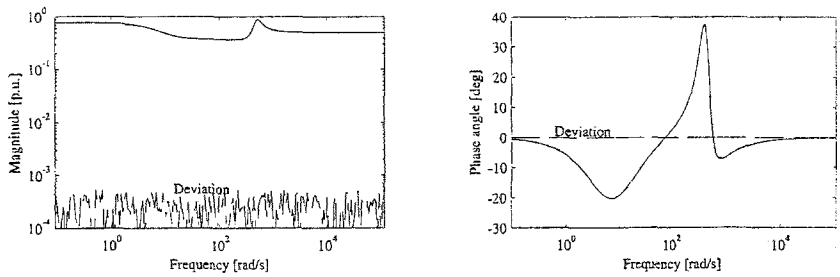

Figure 7. Approximation of rational function contaminated with noise.

The frequency response was calculated numerically from (16) in the interval 10 to 10^5 rad/s. $f(s)$ was then fitted using VFPR with four initial (logarithmically distributed) negative real poles, almost arbitrarily chosen to cover an equal interval of the real axis. The coefficients of the calculated approximation were as follows:

Poles	*Residues*	*Constant term*
−5.0000E+000	2.0000E+000	5.0000E−001
−1.0000E+002 +j5.0000E+002	3.0000E+001 +j4.0000E+001	
−1.0000E+002 −j5.0000E+002	3.0000E+001 −j4.0000E+001	
−1.0000E+005	1.2428E−010	

Thus, all coefficients in (16) have been identified with very high accuracy. The "surplus" pole (−1.0000E+005) has a very small residue (1.24E−10) and does therefore not contribute to the response. The root mean square (RMS) of the deviation was 1.22E−15. Note that real starting poles worked well in this example because the order of fitting is very low. In general, complex starting poles should be used, as explained in Section 3.2.

This example shows that VFPR is capable of identifying the parameters of a rational function from its frequency response. We next demonstrate that the method also works when the frequency response has been contaminated with noise. Figure 7 shows the fitted response when random noise between 0 and 1E−3 has been added to $f(s)$.

The resulting coefficients of the approximation are listed below:

Poles	*Residues*	*Constant term*
−5.0035E+000	1.9996E+000	5.0047E−001
−9.9937E+001 +j5.0002E+002	2.9996E+001 +j3.9983E+001	
−9.9937E+001 −j5.0002E+002	2.9996E+001 −j3.9983E+001	
−1.8308E−002	4.9442E−004	

The coefficients are now slightly in error. This simply reflects the fact that the modified coefficients give a better approximation of the contaminated response than those of the original response.

Similar results were obtained for an 18th-order response [7].

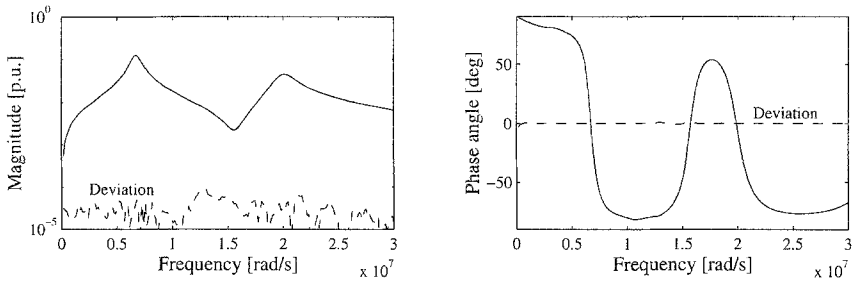

Figure 8. Approximation of measured frequency response (10th-order approximation).

Example 2: Approximation of Measured Transformer Response. When calculating electromagnetic transients in power systems, the frequency variation in electrical parameters should be taken into account. In the case of a transformer, the frequency variation is given as a measured frequency response at its terminals. To include the transformer in a simulation of transients requires the matrix of measured admittance functions to be approximated with rational functions.

As an example, we consider one element of the admittance matrix for a distribution transformer. Figure 8 shows the approximation of the element using 10 poles. The approximation is seen to be quite accurate. Note that the response is contaminated with an unknown amount of measurement errors and contributions from nonlinear effects.

Example 3: Approximation of Calculated Transmission Line Propagation Matrix. In electromagnetic transient studies, transmission lines are modeled using frequency-dependent distributed parameters. The distorting effects of wave propagation between two line ends is taken into account by a propagation matrix, H. This is a square, frequency-dependent matrix with dimension equal to the number of conductors of the line.

Figure 9 shows the fitted elements of one column of H, for an eight-conductor overhead line. Note that all elements were fitted *simultaneously* using 30 poles. This has the effect that all elements get identical poles. The feature of identical poles is desirable because for a given order it leads to computational savings in the time-domain (transient) simulations [4]. Increasing the order led to a further increase in accuracy. Similar results were achieved for the remaining four columns. Note that the "oscillating" behavior in Figure 9 occurs because the elements contain uncompensated time delays.

Example 4: Approximation of Network Response. Time-domain simulations of electromagnetic transients can be very time consuming as a large number of power system components may need to be considered and because the required number of time steps can be very high. To overcome this problem, network reduction techniques [12] are sometimes used, where portions of the network are

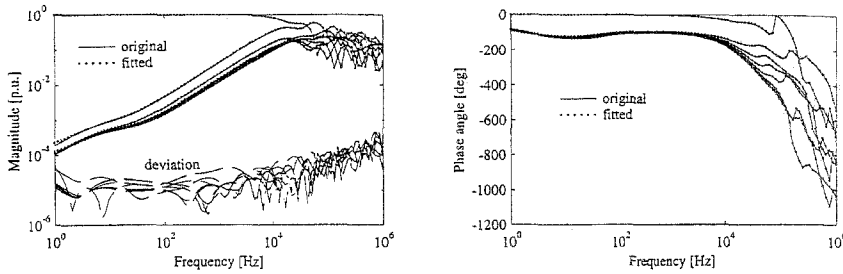

Figure 9. Approximation of one column of a transmission line propagation matrix (30th-order approximation).

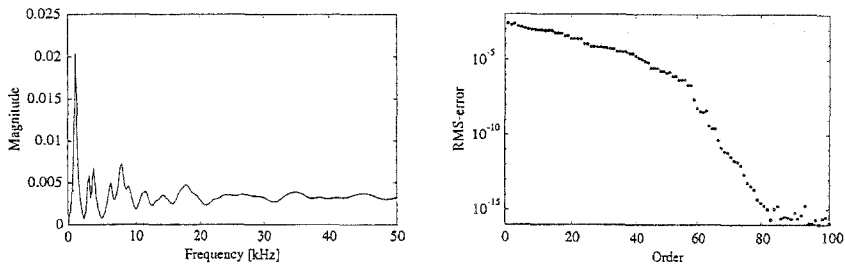

(a) Admittance function

(b) Error of approximation

Figure 10. Approximation of zero sequence admittance function by VFPR. (a) admittance function, (b) error of approximation.

represented by their terminal equivalent (admittance matrix). These techniques require rational approximation of the frequency responses seen at the terminals of the equivalent.

To demonstrate the technique, we consider the zero sequence admittance function for a network of transmission lines, shown in Figure 10a. Figure 10b shows how the RMS error of the approximation by VFPR decreases as the order of the approximation is increased.

The time-domain simulation of power system transients has traditionally been based on trapezoidal integration [2]. Figure 11 shows the time-domain step response calculated by trapezoidal integration when the order of the rational approximation is 50 and 100, respectively. The two responses are virtually identical.

4. Conclusions

The paper has two main parts. In the first part, we analyze the ill conditioning characteristic to the problem of rational fitting. The main conclusions of this

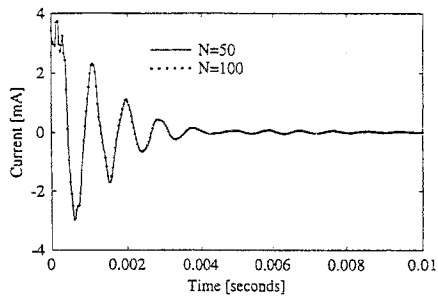

Figure 11. Step response of network equivalent of Figure 10a.

analysis are that in general the poles needed for state equation approximation cannot be located directly because of the ill conditioning, and if one does not have the right poles, then, with the poles at hand, a given (scalar or vector) transfer function cannot be represented in the form of a rational expansion.

The second part of the paper gives a solution to this dilemma. It describes a fitting methodology based on modifying the given transfer function by scaling. This in effect relocates the initial poles to much better new positions. Even though the problem of state equation approximation is both nonlinear and intrinsically ill conditioned, the new method of Vector Fitting by Pole Relocation uses only robust standard methods of numerical linear algebra. It is thus both reliable and accurate.

References

[1] G. Angelidis and A. Semlyen, Direct phase-domain calculation of transmission line transients using two-sided recursions, *IEEE Trans. Power Delivery*, PWRD-10(2), 941–949, April 1995.

[2] H. W. Dommel and W. S. Meyer, Computation of electromagnetic transients, *Proc. IEEE*, 62(7), 983–993, July 1974.

[3] B. Gustavsen and A. Semlyen, Combined phase and modal domain calculation of transmission line transients based on vector fitting, *IEEE Trans. Power Delivery*, PWRD-13(2), 596–604, April 1998.

[4] B. Gustavsen and A. Semlyen, Simulation of transmission line transients using vector fitting and modal decomposition, *IEEE Trans. Power Delivery*, PWRD-13(2), 605–614, April 1998.

[5] B. Gustavsen and A. Semlyen, Application of vector fitting to state equation representation of transformers for simulation of electromagnetic transients, *IEEE Trans. Power Delivery*, PWRD-13(3), 834–842, July 1998.

[6] B. Gustavsen and A. Semlyen, Calculation of transmission line transients using polar decomposition, *IEEE Trans. Power Delivery*, PWRD-13(3), 855–862, July 1998.

[7] B. Gustavsen and A. Semlyen, Rational approximation of frequency domain responses by vector fitting, *IEEE Trans. Power Delivery*, PWRD-14(3), 1052–1061, July 1999.

[8] N. J. Higham, *Accuracy and Stability of Numerical Algorithms*, SIAM, Philadelphia, 1996.

[9] J. R. Marti, Accurate modelling of frequency-dependent transmission lines in electromagnetic transient simulations, *IEEE Trans. Power Apparat. Systems*, PAS-101(1), 147–157, January 1982.

[10] A. Morched, B. Gustavsen, and M. Tartibi, A universal model for accurate calculation of electromagnetic transients on overhead lines and underground cables, *IEEE Trans. Power Delivery*, PWRD-14(3), 1032–1038, July 1999.

[11] A. Morched, L. Marti, and J. Ottevangers, A high frequency transformer model for the EMTP, *IEEE Trans. Power Delivery*, PWRD-8(3), 1615–1626, July 1993.

[12] A. Morched, J. Ottevangers, and L. Marti, Multi-port frequency dependent network equivalents for the EMTP, *IEEE Trans. Power Delivery*, PWRD-8(3), 1402–1412, July 1993.

[13] H. V. Nguyen, H. W. Dommel, and J. R. Marti, Direct phase domain modelling of frequency-dependent overhead transmission lines, *IEEE Trans. Power Delivery*, PWRD-12(3), 1335–1342, July 1997.

[14] T. Noda, N. Nagaoka, and A. Ametani, Further improvements to a phase-domain arma line model in terms of convolution, steady-state initialization, and stability, *IEEE Trans. Power Delivery*, PWRD-12(3), 1327–1334, July 1997.

[15] R. Ober and S. Montgomery, Bilinear transformation of infinite-dimensional state-space systems and balanced realisation of nonrational transfer function, *SIAM J. Control Optim.*, 6, 438–465, 1990.

[16] D. Salamon, Realization theory in Hilbert space, *Math. Syst. Theory*, 21, 147–164, 1989.

[17] A. Semlyen and A. Dabuleanu, Fast and accurate switching transient calculations on transmission lines with ground return using recursive convolutions, *IEEE Trans. Power Apparat. Systems*, PAS-94(2), 561–571, March/April 1975.

[18] A. O. Soysal and A. Semlyen, Practical transfer function estimation and its apllication to wide frequency range representation of transformers, *IEEE Trans. Power Delivery*, PWRD-8(3), 1627–1637, July 1993.

[19] A. O. Soysal and A. Semlyen, State equation approximation of transfer matrices and its application to the phase domain calculation of electromagnetic transients, *IEEE Trans. Power Systems*, PWRS-9(1), 420–428, February 1994.

[20] A. O. Soysal and A. Semlyen, Reduced order transmission line modeling for improved efficiency in the calculation of electromagnetic transients, *IEEE Trans. Power Systems*, PWRS-9(3), 1494–1498, August 1994.